

Rate Constants for 1,5- and 1,6-Hydrogen Atom Transfer Reactions of Mono-, Di-, and Tri-aryl-substituted Donors, Models for Hydrogen Atom Transfers in Polyunsaturated Fatty Acid Radicals

Christopher B. DeZutter, John H. Horner, and Martin Newcomb*

Department of Chemistry, University of Illinois at Chicago, 845 West Taylor Street, Chicago, Illinois 60607

Received: November 9, 2007; In Final Form: December 19, 2007

Rate constants for 1,5- and 1,6-hydrogen atom transfer reactions in models of polyunsaturated fatty acid radicals were measured via laser flash photolysis methods. Photolyses of PTOC (pyridine-2-thioneoxycarbonyl) ester derivatives of carboxylic acids gave primary alkyl radicals that reacted by 1,5-hydrogen transfer from mono-, di-, and tri-aryl-substituted positions or 1,6-hydrogen transfer from di- and tri-aryl-substituted positions to give UV-detectable products. Rate constants for reactions in acetonitrile at room temperature ranged from 1×10^4 to 4×10^6 s⁻¹. The activation energies for a matched pair of 1,5- and 1,6-hydrogen atom transfers giving tri-aryl-substituted radicals were approximately equal, as were the primary kinetic isotope effects, but the 1,5-hydrogen atom transfer reaction was 1 order of magnitude faster at room temperature than the 1,6-hydrogen atom transfer reaction due to a less favorable entropy of activation for the 1,6-transfer reaction. Solvent effects on the rate constants for the 1,5-hydrogen atom transfer reaction of the 2-[2-(diphenylmethyl)phenyl]ethyl radical at ambient temperature were as large as a factor of 2 with the reaction increasing in rate in lower polarity solvents. Hybrid density functional theory computations for the 1,5- and 1,6-hydrogen atom transfers of the tri-aryl-substituted donors were in qualitative agreement with the experimental results.

Hydrogen atom transfer reactions are important processes of radical chemistry in synthetic applications, polymerizations, and biological reactions. Inherently fast hydrogen atom transfers occur from carbon atoms to oxygen- and positively charged nitrogen-centered radicals due to the exothermicity of the reactions, but hydrogen atom transfers from a carbon atom to a carbon-centered radical are considerably slower in comparison, even when the reaction enthalpies are comparable.^{1,2} Because of the fundamental nature of hydrogen atom transfer reactions, their rate constants have been addressed by numerous empirical and ab initio calculation methods dating from the earliest approaches to understanding chemical dynamics^{3–6} to recent studies.⁷ Much of the focus in hydrogen-transfer reaction kinetics has been on intermolecular reactions. For intramolecular hydrogen atom transfer reactions, considerable information has been gathered for reactions of oxygen-centered radicals, but reactions of carbon-centered radicals are less well studied.^{2,8}

The rates of hydrogen atom transfer reactions in radicals derived from polyunsaturated fatty acids (PUFAs) attracted our interest. Several radical processes are important for PUFAs, including oxidations by cyclooxygenase (COX) enzymes,⁹ isomerization reactions of cis double bonds,¹⁰ and autoxidation reactions.¹¹ Some of these processes involve multiple steps where hydrogen atom transfer reactions can compete with other intramolecular processes, such as C–C bond-forming reactions, and with intermolecular reactions, such as reaction with molecular oxygen.¹² Decreases of the bond dissociation energies (BDEs) of PUFA C–H bonds that are allylic or doubly allylic are expected to increase the rates of hydrogen atom transfer reactions from these sites to carbon-centered radicals to levels that are competitive with those of other reactions of carbon radicals. It is also to be expected that subtle differences in

enthalpic and entropic factors for the H-atom transfer reactions can be manifested in pronounced changes in product distributions.

In this work, we report kinetic studies for intramolecular 1,5- and 1,6-hydrogen atom transfer reactions in models for PUFA radicals that contain aryl groups as surrogates for double bonds measured directly by laser flash photolysis (LFP) methods. 1,5-Hydrogen transfer from a monostabilized position is a relatively slow process, whereas 1,5- and 1,6-hydrogen transfers from doubly stabilized positions, equivalent to doubly allylic positions in PUFAs, are relatively facile reactions with rate constants in the range of 10^4 – 10^5 s⁻¹ at ambient temperature. Hydrogen atom transfers from triply stabilized positions are fast, with the rate constant for the 1,5-hydrogen transfer reaching 4×10^6 s⁻¹ at ambient temperature.

Experimental Methods

Radical Precursors. The synthetic reactions for preparation of the radical precursors are detailed in the Supporting Information. In brief, appropriate carboxylic acids were synthesized and then converted to radical precursors that are mixed anhydrides of the carboxylic acid and the thiohydroxamic acid *N*-hydroxypyridine-2-thione by employing a dicyclohexylcarbodiimide (DCC)-activated coupling reaction. These radical precursors, trivially known as PTOC (for pyridine-2-thioneoxycarbonyl) esters,¹³ decomposed thermally on standing and when exposed to light, but they could be isolated by column chromatography with partial decomposition by methods previously reported.^{14,15} From the NMR spectra of the PTOC esters (see Supporting Information), we concluded that **1a** was $\geq 95\%$ pure and **1b–1e** were $\geq 98\%$ pure.

Kinetic Studies. Laser flash photolysis kinetic studies were performed on Applied Photophysics LK50 and LK60 instru-

* Corresponding author: e-mail men@uic.edu.

ments by use of 355 nm light from a Continuum or a Quantel Nd:YAG laser, respectively. The methods generally followed reported procedures.^{16,17} Solutions of the PTOC ester precursors were prepared with total absorbances of ca. 0.5 au at 355 nm and placed in a jacketed addition funnel. The solutions were deoxygenated by helium gas sparging and allowed to flow through the reaction flow cell. Data was acquired at 5 nm intervals by use of photomultiplier tubes with 2 ns response times. For variable-temperature studies, a temperature-controlled solution was circulated through the jacket of the addition funnel and a block that held the flow cell. Temperatures were measured with a thermocouple placed in the flowing stream ca. 1 cm above the light irradiation zone. Kinetic data acquired at 335 nm was solved as single-exponential (growth) or double-exponential (growth plus decay) functions. Complete kinetic data are given in the Supporting Information.

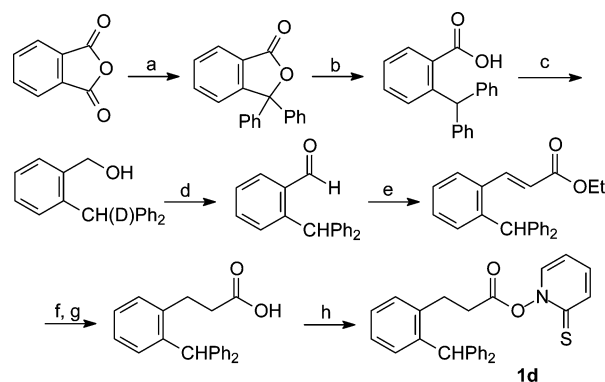
Computational Details. Theoretical calculations at the B3LYP/6-31G(d) level were carried out with Gaussian 98¹⁸ to evaluate the isotope effects for the 1,5- and 1,6-hydrogen transfers in radicals **3d** and **3e**, respectively. Minimized structures for **3d**, **4d**, **3e**, and **4e** were located, along with the transition states connecting **3d** to **4d** and **3e** to **4e**. Frequency calculations were carried out on the deuterated and undeuterated isomers. In the deuterated cases, a single deuterium atom was introduced, corresponding to the deuterium atom being transferred. The scaled vibrational frequencies for monodeuterated and undeuterated transition states and for **3d** and **3e** (undeuterated and monodeuterated) were used as input for the Biegeleisen equation.¹⁹ Detailed results are in the Supporting Information.

Results and Discussion

Allylic and benzylic C–H bonds have similar bond dissociation energies (BDEs),²⁰ and early computational studies often took advantage of this fact and modeled phenyl groups with C–C double bonds. In this work, we reversed the approach and modeled C–C double bonds with phenyl groups, which provides several advantages. The aryl-substituted radical products have strongly absorbing chromophores in a region in the UV–visible spectrum that has little interfering absorbance, thus permitting direct kinetic studies with UV–visible spectroscopy. The possible isomerization of a double bond is not an issue with aryl group substitution. Most importantly, radical cyclizations onto alkenyl positions will compete with or overwhelm hydrogen atom transfer reactions in alkene radicals,²¹ even when the radical cyclization is relatively slow, as in a 4-exo cyclization,²² but intramolecular radical addition reactions to aryl groups are much slower and do not interfere with the reactions we studied here. For example, the 3-exo cyclization reaction of a primary radical center onto a phenyl group in the 2-methyl-2-phenylpropyl radical, which is the rate-limiting step in the neophyl rearrangement, is 2–4 orders of magnitude slower than the reactions studied in this work.²³

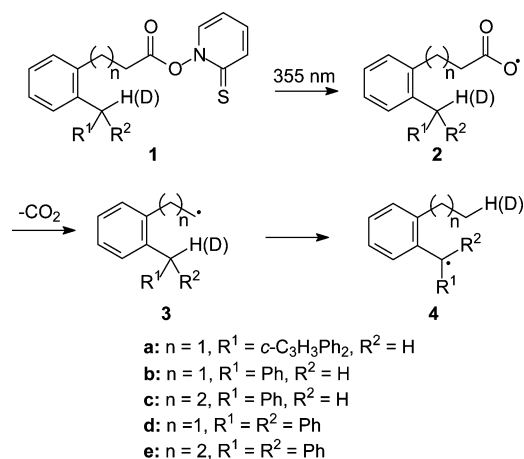
Radicals and Radical Precursors. The radical precursors were mixed anhydrides of carboxylic acids and the thiohydroxamic acid *N*-hydroxypyridine-2-thione. These intermediates were developed for synthetic purposes by Barton et al.¹³ and are known by the trivial name of PTOC esters, where the acronym is for pyridine-2-thioneoxycarbonyl. The synthetic details are in the Supporting Information, and a representative synthesis of one of the PTOC ester precursors is shown in Scheme 1. The synthetic sequence is routine, with the possible exception of the first step, which is a selective addition of Grignard reagent that has precedence.²⁴ In the original synthetic developments,

SCHEME 1^a



^a (a) PhMgBr, Et₂O, 48%; (b) H₂, Pd/C, EtOAc, 97%; (c) LiAlH₄, Et₂O, 87%; (d) PCC, CH₂Cl₂, 92%; (e) Ph₃P=CHCO₂Et, CH₂Cl₂, 99%; (f) Pd/C, EtOAc, 99%; (g) LiOH, H₂O/THF, 89%; (h) 1-hydroxy-1H-pyridine-2-thione, DCC, CH₂Cl₂, 76%.

SCHEME 2

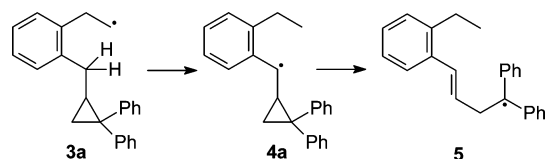


PTOC esters were not isolated,¹³ but they can be purified by column chromatography on silica gel with some decomposition.¹⁴ The PTOC esters used in this work were purified by chromatography and judged by NMR spectroscopy to be $\geq 98\%$ pure in all but one case, **1a**, where the precursor was $\geq 95\%$ pure. NMR spectra of the PTOC esters are in Supporting Information.

Scheme 2 shows the PTOC esters and radicals studied in this work. Photolysis of a PTOC ester (**1**) with 355 nm laser light resulted in efficient cleavage of the weak O–N bond to give an acyloxyl radical (**2**) and the pyridine-2-thiyl radical as a byproduct. Fast decarboxylation of radicals **2** (subnanosecond) gave the desired radicals **3**, and intramolecular hydrogen transfer in radicals **3** gave product radicals **4**. For the tri-aryl-substituted systems, radicals **3d** and **3e**, the kinetics of deuterium transfers in radicals **3d(D)** and **3e(D)** also were measured to give kinetic isotope effects. For the other radicals studied, the deuterium-atom transfer reactions were so slow that competing radical–radical reactions were important, and kinetic isotope effects could not be determined with good precision.

Radicals **3b**–**3e** gave di-aryl- and tri-aryl-substituted product radicals **4** that could be detected readily due to their strong UV absorbances (see below). The analogous product in a mono-substituted system, benzylic radical **4a**, was expected to have a relatively weak absorbance with λ_{max} at about 310 nm.²⁵ In order to obtain stronger signals for the product radical in the monosubstituted system, we used the radical reporter method²⁶ shown in Scheme 3. Thus, hydrogen transfer in radical **3a** gave

SCHEME 3



product radical **4a**, and fast ring opening of **4a** gave radical **5**, which contains a strong chromophore due to the diarylmethyl radical. The ring opening of radical **4a** must have a rate constant exceeding $1 \times 10^8 \text{ s}^{-1}$ at ambient temperature by analogy to related systems,^{27–30} and the rate constant for the fast conversion of **4a** to **5** will not be convoluted with the rate constant for hydrogen atom transfer in radical **3a**.

Spectroscopy. The sequence of reactions occurring in the laser flash photolysis (LFP) studies was similar for all radicals studied, as illustrated in Scheme 2. Irradiation of the PTOC ester precursors gives radicals **2**, and the byproduct of the photolysis is the pyridine-2-thiyl radical. The latter species has a long-wavelength absorbance with $\lambda_{\text{max}} = 490 \text{ nm}$,³¹ and it can be used to quantify the concentration of radicals formed from the laser pulse. Because radicals **2** rapidly decarboxylated to give radicals **3**, the 7 ns laser pulse gave radicals **3** and the pyridine-2-thiyl radical “instantly” on our experimental time scale. Rate constants for the H-atom transfer reactions of radicals **3** were measured directly by following the formation of radicals **4**.

In the kinetic studies with UV–visible spectroscopy for detection, destruction of the PTOC esters by the laser pulse resulted in immediate bleaching of the signal from these precursors, which have a long wavelength λ_{max} at ca. 360 nm. The initially formed alkyl radicals do not have absorbances at wavelengths greater than 300 nm. Signals from the diarylmethyl or triarylmethyl product radicals with $\lambda_{\text{max}} \approx 335 \text{ nm}$ ²⁵ grew in with time. Figure 1, which is typical, shows growth of the diarylmethyl radical **4b** from reaction of radical **3b**. In this representation, the initial spectrum observed after the laser pulse was subtracted from subsequent spectra; species forming with time have positive signals, and those decaying with time have negative signals. In addition to the growth of radical **4b** with $\lambda_{\text{max}} = 335 \text{ nm}$, decay of the pyridine-2-thiyl radical with $\lambda_{\text{max}} = 490 \text{ nm}$ is apparent.

Kinetics. Rate constants for reactions of the alkyl radicals **3** in acetonitrile were measured. Detailed kinetic results are in the Supporting Information, and observed rate constants for reactions at 20 °C are listed in Table 1. For the fast-reacting radical **3d**, the 1,5-hydrogen atom transfer reaction that gave product **4d** had $k = 3.8 \times 10^6 \text{ s}^{-1}$ at 20 °C, and this was the only important reaction. For other radicals, competing radical reactions became increasingly important as the rate constants for the hydrogen transfer reactions decreased. The third column in Table 1 lists corrected rate constants for the H-atom transfer reactions at 20 °C where we have subtracted from the observed rate constant an estimated contribution for other reactions of the precursor radicals as discussed later.

One trend in the kinetics is that increasing the stability of the product radical by increasing the delocalization from two to three aryl groups resulted in a 20–30-fold kinetic acceleration for both series of radicals. A similar difference in rate constants was found for the mono- and di-aryl-substituted systems **3a** and **3b**. The cyclopropyl reporter group in radical **3a** was expected to have a modest accelerating effect on the H-atom transfer reaction because C–H bonds adjacent to a cyclopropane ring are weakened by about 3 kcal/mol,³⁰ and this appears to be the case. Specifically, the reaction of radical **3a** is 1 order of

TABLE 1: Rate Constants for Hydrogen-Atom Transfer Reactions in Acetonitrile at 20 °C

radical	k_{obs}^a (s^{-1})	$k_{\text{H-atom}}^b$ (s^{-1})
3a	2.3×10^4	1.5×10^4
3b	1.4×10^5	1.3×10^5
3c	2.5×10^4	1.5×10^4
3d	3.8×10^6	3.8×10^6
3d(D) ^c	5.4×10^5	5.3×10^5
3e	3.5×10^5	3.4×10^5
3e(D) ^d	4.7×10^4	4×10^4

^a Observed first-order rate constants at 20 ± 1 °C. ^b Corrected rate constant for hydrogen atom transfer determined as described in the text. ^c Deuterated version of radical **3d**; for radical **3d**, $k_{\text{H}}/k_{\text{D}} = 7.2$. ^d Deuterated version of radical **3e**; for radical **3e**, $k_{\text{H}}/k_{\text{D}} = 8.5$.

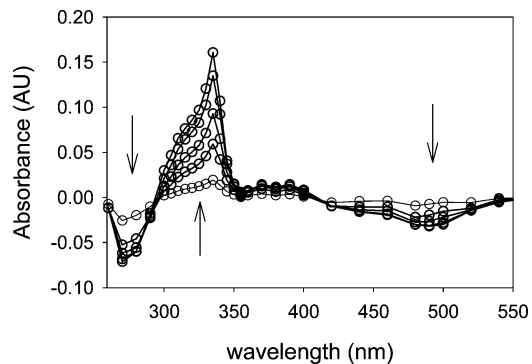


Figure 1. Time-resolved spectrum from reaction of radical **3b**. The time slices are at 1.1, 3.4, 6.1, 12, and 25 μs . Diarylmethyl radical product **4b** with $\lambda_{\text{max}} = 335 \text{ nm}$ is growing in, and the pyridine-2-thiyl radical with $\lambda_{\text{max}} \approx 280 \text{ nm}$ and $\lambda_{\text{max}} = 490 \text{ nm}$ is decaying.

magnitude faster than the 1,5-hydrogen atom transfer reaction in the 6-heptenyl radical,²¹ which has an estimated rate constant of ca. 1000 s^{-1} at 25 °C when one adjusts for the currently accepted rate constant for reaction of Bu_3SnH with a primary alkyl radical.³²

The rate constants for the slower hydrogen atom transfer reactions were corrected to remove kinetic contributions from competing reactions. The importance of competing reactions was indicated by the reduction of signal growth for the product radicals formed in the relatively slow hydrogen transfer reactions, most obviously in reactions of radicals **3a**, **3c**, and **3e(D)**. The three di-aryl-substituted radical products **4b**, **4c**, and **5** should have comparable extinction coefficients at λ_{max} , and the absorbances for the two triaryl radical products **4d** and **4e** should be similar to one another. In Figure 2A, the signals at 335 nm showing bleaching of the precursors and growth of the triarylmethyl product radicals **4d** and **4e** are compared. The amount of signal growth at 335 nm is similar for the two radicals, indicating that competing reactions of the precursor radicals **3d** and **3e** were minor in both cases. In Figure 2B, however, where we compare the signal growth for diarylmethyl radical products **4b** and **4c**, the signal from the 1,6-hydrogen transfer reaction of radical **3c** (giving **4c**) is considerably smaller than that from the 1,5-hydrogen transfer reaction of radical **3b** (giving **4b**). This indicates that competing reactions were a significant component of the total reactions for the relatively slow 1,6-hydrogen transfer of radical **3c**.

The observed first-order rate constants are the sum of the rate constants for all processes that consume the reacting radicals, and one expected that the contribution to the total kinetics arising from side-reactions could be significant for the slow-reacting radicals **3a**, **3c**, and **3f(D)**. Possible competing reactions are radical–radical coupling and disproportionation reactions, reactions with residual oxygen, and reactions with

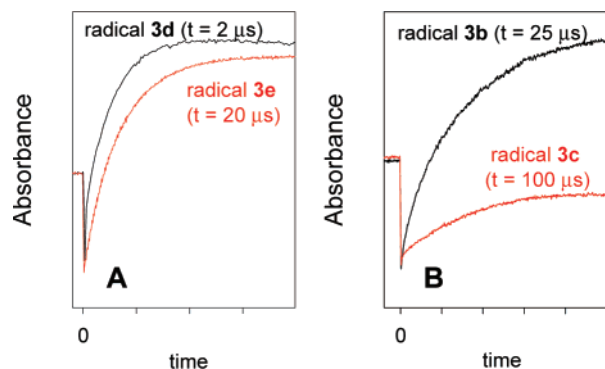


Figure 2. Kinetic traces at 335 nm for reactions of various radicals at ambient temperature: (A) formation of triarylmethyl radical products **4d** from radical **3d** (black) and **4e** from radical **3e** (red); (B) formation of diarylmethyl radical products **4b** from radical **3b** (black) and **4c** from radical **3c** (red). Note that the time scales are different for each radical with the total times for the traces shown following the radical label. The traces in panel B were normalized such that the initial bleaching had the same intensity for both radicals.

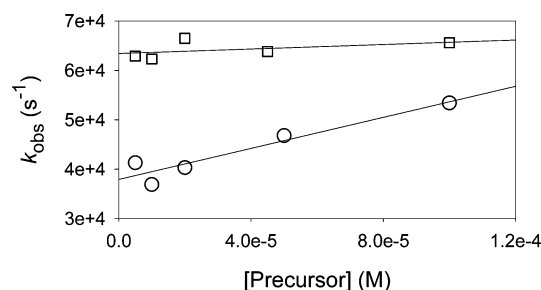


Figure 3. Concentration effects on rate constants for reactions of radical **3e(D)** at ambient temperature in acetonitrile (O) and in trifluorotoluene (□).

solvent. Another potential competing reaction is addition of the radical to another molecule of the PTOC ester precursor, but this reaction can be excluded because the rate constant is ca. $1 \times 10^6 \text{ M}^{-1} \text{ s}^{-1}$ at room temperature³³ and small concentrations of PTOC precursors **1** (ca. $5 \times 10^{-5} \text{ M}$) were used in the LFP studies.

Each radical **3** is a primary alkyl radical, and the rates of the competing radical reactions should be similar for all reactions we studied. Thus, the kinetic contributions from the competing processes should add a constant absolute amount to the total kinetic values as long as the concentrations of radicals initially produced are similar. In practice, for the observed rate constants reported in Table 1, the concentrations of PTOC ester precursors were approximately equal.

We estimated the amount of radical–radical reactions occurring for the relatively slow-reacting radical **3e(D)**. This radical was employed because the triarylmethyl radical product **4e** has a strong absorbance, and we wished to measure kinetics at low radical concentrations. Radical **3e(D)** was produced at room temperature in solutions with varying concentrations of PTOC ester precursor. The kinetic results are shown graphically in Figure 3. As the concentration of precursor, and also of radical **3e(D)**, decreased, the observed rate constants decreased somewhat because radical–radical reactions became less important.

Extrapolation of the results for **3e(D)** in acetonitrile to infinite dilution gave a value for reaction of this radical at room temperature of $k = 4 \times 10^4 \text{ s}^{-1}$ in acetonitrile solvent. The dilution study allowed us to factor out the effect of radical–radical reactions (couplings and disproportionations), but reactions of radicals with residual oxygen and with solvent are still included in the kinetic values. The extrapolated rate constant

TABLE 2: Rate Constants for Hydrogen-Atom Transfer Reactions of Radical **3d in Various Solvents^a**

solvent	$k_{\text{H-atom}}^b$ (s^{-1})	ϵ^c	$E_{\text{T}}(30)^d$
cyclohexane	7.7×10^6	2.0	30.9
THF	5.8×10^6	7.6	37.4
TFT ^e	6.2×10^6	9.0	38.5
acetonitrile	4.2×10^6	36	45.6
2-propanol	6.7×10^6	20	48.4
methanol	5.9×10^6	33	55.4
TFE ^f	5.1×10^6	27	59.8

^a First-order rate constants for hydrogen atom transfer at 23 ± 1 °C; the errors are <2% of the reported value. ^b The rate constants for acetonitrile and trifluorotoluene are calculated from the temperature-dependent functions in Table 3; other rate constants are measured values. ^c Relative permittivity (dielectric constant) at 25 °C from refs 34 and 35. ^d $E_{\text{T}}(30)$ solvatochromatic value from ref 36. ^e TFT, α,α,α -trifluorotoluene. ^f TFE, 2,2,2-trifluoroethanol.

for reaction of **3e(D)** at infinite dilution in CH_3CN solution was smaller than the rate constant for reaction of a $5 \times 10^{-5} \text{ M}$ solution by ca. $1 \times 10^4 \text{ s}^{-1}$, and we corrected the observed rate constants by subtracting this value from each observed kinetic value. The corrected rate constants are listed in the third column of Table 1.

Solvent Effects. The dilution study for radical **3e(D)** was repeated in α,α,α -trifluorotoluene (TFT) solvent in an attempt to determine whether reaction of the primary alkyl radical with acetonitrile solvent was significant. If it were, then the total reaction rate in TFT should be smaller than that found in CH_3CN . Surprisingly, the rate constant for reaction in TFT was 50% larger than that for reaction in acetonitrile, $k = 6 \times 10^4 \text{ s}^{-1}$ at ambient temperature. Dilution study results in TFT, which are included in Figure 3, indicated that there was only a small contribution of radical–radical reactions to the total kinetics for **3e(D)** in this solvent. Furthermore, good signal intensity for the product radical **4e** suggested that reaction of **3e(D)** with the solvent or with residual oxygen was no more prevalent in TFT than in CH_3CN . The only logical conclusion for the difference in rate constants was that there was a modest solvent effect on the rate of the H-atom transfer reaction.

The apparent kinetic solvent effect for the hydrogen atom transfer reaction of radical **3e(D)** was confirmed by studying the fastest reaction in the series, the 1,5-H atom transfer of radical **3d**, in several solvents. Because radical **3d** reacts rapidly, competing radical reactions cannot contribute significantly to the total kinetics of the reaction. Therefore, changes in the rate constants should reflect only solvent effects. Rate constants for reaction of **3d** in different solvents are listed in Table 2 with the solvent dielectric constants^{34,35} and $E_{\text{T}}(30)$ solvent polarity values.³⁶ The rate constants varied by nearly a factor of 2, and in agreement with the results for radical **3e(D)**, the rate constant for reaction of **3d** in TFT was a factor of 1.5 times as great as that in CH_3CN .

The solvent effects on the rate constants for reaction of **3d** were not large in comparison to those found for polar reactions, but they are noteworthy for a radical reaction. Kinetic solvent effects are known for radical reactions that have large changes in polarities as found with additions of alkyl radicals to acrylates,^{37,38} aminium cation radical reactions,³⁹ decarbonylations of acyl radicals,⁴⁰ and reactions of thiols with methoxy-substituted radicals.⁴¹ Typically, however, the assumption is that most radical reactions will not display kinetic solvent effects, and this has been demonstrated in some cases, such as in nitroxide radical trapping reactions.⁴² Although not necessarily obvious, the aryl-substituted product radicals **4** in this work do have larger dipoles than the primary alkyl radical reactants **3**,

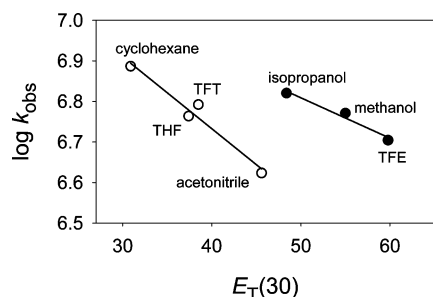


Figure 4. Rate constants for reactions of radical **3d** at 23 °C as a function of solvent polarity. The lines are regression fits for the two sets of data.

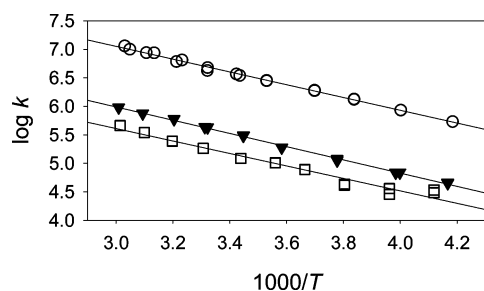


Figure 5. Temperature-dependent kinetics for reactions of radicals **3b** (\square), **3d** (\circ), and **3e** (\blacktriangledown) in acetonitrile. The lines are the Arrhenius functions in Table 4.

TABLE 3: Arrhenius Functions for Intramolecular Hydrogen Atom Transfer Reactions^a

radical	$\log A$	E_a (kcal/mol)	k_{20}^b (s ⁻¹)
3b	8.9 ± 0.4	5.0 ± 0.5	1.4×10^5
3d	10.41 ± 0.11	5.12 ± 0.15	3.9×10^6
3d(D)^c	10.05 ± 0.17	5.81 ± 0.23	5.2×10^5
3e	9.47 ± 0.12	5.31 ± 0.15	3.2×10^5
3e(D)^d	9.0 ± 0.5	5.84 ± 0.6	4.4×10^4
3d (TFT)^e	11.0 ± 0.2	5.7 ± 0.3	5.5×10^6

^a For reactions in acetonitrile unless noted. Listed errors are at 2σ .

^b Calculated rate constant at 20 °C. ^c For **3d**, the calculated KIE at 20 °C is $k_H/k_D = 7.5$. ^d For **3e**, the calculated KIE at 20 °C is $k_H/k_D = 7.3$.

^e Reaction in trifluorotoluene solvent.

and computations for radicals **3d** and **3e** indicated that the transition states for the hydrogen atom transfer reactions are more polarized than the initial radicals (see below). Thus, one might predict that increasing solvent polarity would accelerate the hydrogen atom transfer reactions. The observed effects are the opposite of that prediction, however, as shown in Figure 4 where the rate constants are plotted as a log function of the solvent polarities as measured on the $E_T(30)$ solvent polarity scale.³⁶ The solvents can be divided into two groups, non-hydrogen-bonding and hydrogen-bonding. Within each group, the rate constants for the hydrogen atom transfer reactions decrease with increasing solvent polarity. For acetonitrile and TFT, the seemingly counterintuitive kinetics results were found to be due to compensating enthalpic and entropic changes; the enthalpy of activation in the more polar solvent was indeed smaller than that in the less polar solvent, but the effect due to the entropy of activation was greater than the enthalpy effect (see below).

Activation Parameters. Variable-temperature kinetic studies were conducted for radicals **3b**, **3d**, and **3e** (Figure 5) and isotopomers **3d(D)** and **3e(D)**. The resulting Arrhenius parameters are listed in Table 3. The H-atom abstraction reactions are the major processes for these radicals, and systematic errors in the Arrhenius function parameters due to competing reactions should be small. Analysis of the temperature-dependent kinetic

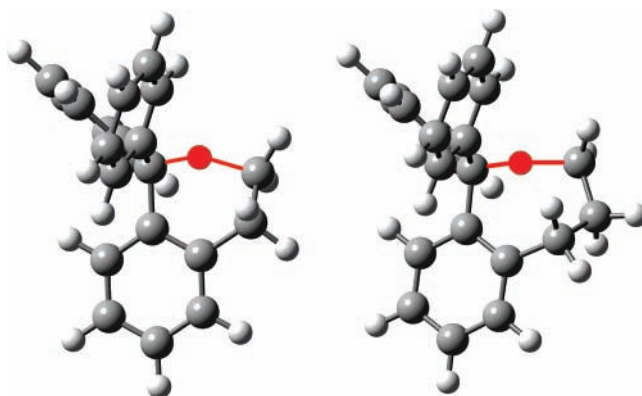


Figure 6. Transition structures for hydrogen atom transfers in radicals **3d** (left) and **3e** (right) at the B3LYP/6-31(d) level. The migrating hydrogen atoms are colored red and shown as bonded to both the abstracting and donating carbon atoms.

TABLE 4: Computed Relative Energies for Hydrogen Atom and Deuterium Atom Transfer Reactions in Radicals **3d and **3e**^a**

system	reactant	TS	product
3d \rightarrow 4d	0	6.3	-24.8
3d(D) \rightarrow 4d	0	7.3	-24.6
3d \rightarrow 4e	0	6.4	-26.3
3e(D) \rightarrow 4e	0	7.4	-26.1

^a Relative zero-point corrected energies are given in kilocalories per mole.

data for the slower radical reactions is possible, but such analyses were not performed because the results would have large degrees of uncertainty due to the requirement that the kinetic contributions from competing reactions be estimated for each temperature. In fact, the small $\log A$ value and large relative errors in the Arrhenius parameters for radical **3b** indicate that the kinetic values for this radical contain relatively constant systematic errors that give increasingly larger percent errors for the low-temperature kinetic values and, hence, artificially small E_a and $\log A$ values.

The Arrhenius function for reaction of radical **3d** in trifluorotoluene (TFT) also was determined, and significant differences were found in the activation parameters for reactions of radical **3d** in this solvent versus acetonitrile. Compensating entropic and enthalpic solvent effects were apparent. The activation energy was reduced in the more polar solvent acetonitrile, as one would predict on the basis of increased polarity in the transition state of the reaction, but the entropic penalty was increased in the more polar solvent (smaller $\log A$ term). Our conjecture is that the increased entropy penalty in acetonitrile reflects increasing order for the polar solvent molecules around the transition state in response to the increasing polarization of the reactant during the course of the reaction.

Computational Results. The hydrogen atom transfer reactions of radicals **3d** and **3e** also were studied computationally at the B3LYP/6-31G(d) level of theory. A very recent report demonstrated that enthalpies of radical reactions calculated at this level can be inaccurate,⁴³ but our primary objective was to compare the activation energies and kinetic isotope effects for quite similar reactions. Despite the caveat, the calculated enthalpies of the reactions and the activation enthalpies were close to the experimentally measured values.

Figure 6 shows the transition states for the H-atom transfer reactions in radicals **3d** and **3e**. In the 1,5-transfer in radical **3d**, the C-H-C angle for the transferring hydrogen atom is 152°, and the corresponding angle for the 1,6-transfer in radical

3e is 171°. The energies of the transition states and the products for these two reactions are listed in Table 4. The computations found nearly equal energy differences for the reactants and transition states for the two radicals. In that regard, the excellent agreement between computed and experimental results is noteworthy. The differences in experimental rate constants for the 1,5- and 1,6-hydrogen atom transfer reactions were due only to the entropies of activation; the activation energies were equal within experimental errors as shown in Table 3.

Kinetic isotope effects for the reactions of **3d** and **3e** were calculated with the Bieleisen equation as described by Olson et al.¹⁹ For reactions at 20 °C, the predicted KIE for radical **3d** and **3d(D)** was $k_H/k_D = 5.6$ (observed $k_H/k_D = 7.2$). For radical **3e** and **4e(D)** at 20 °C, the predicted KIE was $k_H/k_D = 6.3$ (observed $k_H/k_D = 8.5$). These values are in reasonable agreement with the experimental values, and we note that the reaction of radical **4e(D)** is so slow that the experimental rate constant includes a contribution from other reactions.

Conclusion

On the basis of the BDE similarities between allylic and benzylic C–H bonds,²⁰ the kinetic values found in this work should be good approximations for related allylic systems. The 1,5-hydrogen transfer in the mono-aryl-substituted radical **3a** is slow relative to other radical reactions we studied, but its rate constant is in the low range of those for reactions of PUFA radicals.⁴⁴ The rate constants for hydrogen transfer in the di-aryl-substituted radicals **3b** and **3c** are comparable to those for reactions of PUFA radicals, and the tri-aryl-substituted systems **3d** and **3e** have rate constants that are at the upper end of those for PUFA radicals. These observations illustrate that reactions forming pentadienyl radicals by hydrogen atom abstraction from doubly allylic positions can compete with other reactions of PUFA radicals.

The solvent effects found for the hydrogen atom transfer reaction of radical **3d** are noteworthy. They are large enough that the polarity and hydrogen-bonding environment in the vicinity of the radical could influence the product distribution, and this demonstrates an unexpected manner by which enzymes could influence product distributions in radical reactions.

Acknowledgment. This work was supported by a grant from the National Science Foundation (CHE-0601857).

Supporting Information Available: Complete kinetic results, synthetic details, computational results, and NMR spectra of the radical precursors. This material is available free of charge via the Internet at <http://pubs.acs.org>.

References and Notes

- Zavitsas, A. A.; Melikian, A. A. *J. Am. Chem. Soc.* **1975**, *97*, 2757–2763.
- Feray, L.; Kuznetsov, N.; Renaud, P. In *Radicals in Organic Synthesis*; Renaud, P., Sibi, M. P., Eds.; Wiley-VCH: Weinheim, Germany, 2001; Vol. 2, pp 246–278.
- Eyring, H.; Polanyi, M. Z. *Phys. Chem. B* **1931**, *12*, 279–311.
- Evans, M. G.; Polanyi, M. *Trans. Faraday Soc.* **1935**, *31*, 875–894.
- Evans, M. G.; Polanyi, M. *Trans. Faraday Soc.* **1938**, *34*, 11–24.
- Polanyi, J. C. *Acc. Chem. Res.* **1972**, *5*, 161–168.
- Zavitsas, A. A.; Chatgililoglu, C. *J. Am. Chem. Soc.* **1995**, *117*, 10645–10654.
- Beckwith, A. L. J.; Ingold, K. U. In *Rearrangements in Ground and Excited States*; de Mayo, P., Ed.; Academic: New York, 1980; Vol. 1, pp 161–310.
- Rouzer, C. A.; Marnett, L. J. *Chem. Rev.* **2003**, *103*, 2239–2304.
- Chatgililoglu, C.; Ferreri, C. *Acc. Chem. Res.* **2005**, *38*, 441–448.
- Yin, H.; Porter, N. A. *Antioxid. Redox Signaling* **2005**, *7*, 170–184.
- Mukherjee, A.; Brinkley, D. W.; Chang, K. M.; Roth, J. P. *Biochemistry* **2007**, *46*, 3975–3989.
- Barton, D. H. R.; Crich, D.; Motherwell, W. B. *Tetrahedron* **1985**, *41*, 3901–3924.
- Ha, C.; Horner, J. H.; Newcomb, M.; Varick, T. R.; Arnold, B. R.; Luszytk, J. *J. Org. Chem.* **1993**, *58*, 1194–1198.
- Johnson, C. C.; Horner, J. H.; Tronche, C.; Newcomb, M. *J. Am. Chem. Soc.* **1995**, *117*, 1684–1687.
- Newcomb, M.; Horner, J. H.; Filipkowski, M. A.; Ha, C.; Park, S. U. *J. Am. Chem. Soc.* **1995**, *117*, 3674–3684.
- Horner, J. H.; Tanaka, N.; Newcomb, M. *J. Am. Chem. Soc.* **1998**, *120*, 10379–10390.
- Frisch, M. J.; Trucks, G. W.; Schlegel, H. B.; Scuseria, G. E.; Robb, M. A.; Cheeseman, J. R.; Montgomery, J. A., Jr.; Vreven, T.; Kudin, K. N.; Burant, J. C.; Millam, J. M.; Iyengar, S. S.; Tomasi, J.; Barone, V.; Mennucci, B.; Cossi, M.; Scalmani, G.; Rega, N.; Petersson, G. A.; Nakatsuji, H.; Hada, M.; Ehara, M.; Toyota, K.; Fukuda, R.; Hasegawa, J.; Ishida, M.; Nakajima, T.; Honda, Y.; Kitao, O.; Nakai, H.; Klene, M.; Li, X.; Knox, J. E.; Hratchian, H. P.; Cross, J. B.; Bakken, V.; Adamo, C.; Jaramillo, J.; Gomperts, R.; Stratmann, R. E.; Yazyev, O.; Austin, A. J.; Cammi, R.; Pomelli, C.; Ochterski, J. W.; Ayala, P. Y.; Morokuma, K.; Voth, G. A.; Salvador, P.; Dannenberg, J. J.; Zakrzewski, V. G.; Dapprich, S.; Daniels, A. D.; Strain, M. C.; Farkas, O.; Malick, D. K.; Rabuck, A. D.; Raghavachari, K.; Foresman, J. B.; Ortiz, J. V.; Cui, Q.; Baboul, A. G.; Clifford, S.; Cioslowski, J.; Stefanov, B. B.; Liu, G.; Liashenko, A.; Piskorz, P.; Komaromi, I.; Martin, R. L.; Fox, D. J.; Keith, T.; Al-Laham, M. A.; Peng, C. Y.; Nanayakkara, A.; Challacombe, M.; Gill, P. M. W.; Johnson, B.; Chen, W.; Wong, M. W.; Gonzalez, C.; Pople, J. A. *Gaussian 98*, Revision A.9; Gaussian, Inc.: Pittsburgh, PA, 1998.
- Olson, L. P.; Niwayama, S.; Yoo, H. Y.; Houk, K. N.; Harris, N. J.; Gajewski, J. J. *J. Am. Chem. Soc.* **1996**, *118*, 886–892.
- Luo, Y.-R. *Handbook of Bond Dissociation Energies in Organic Compounds*; CRC Press: Boca Raton, FL, 2003.
- Beckwith, A. L. J.; Moad, G. *J. Chem. Soc., Chem. Commun.* **1974**, 472–473.
- Park, S.-U.; Varick, T. R.; Newcomb, M. *Tetrahedron Lett.* **1990**, *31*, 2975–2978.
- Franz, J. A.; Barrows, R. D.; Camaioni, D. M. *J. Am. Chem. Soc.* **1984**, *106*, 3964–3967.
- Geyer, B. P. *J. Am. Chem. Soc.* **1942**, *64*, 2226–2227.
- Chatgililoglu, C. In *Handbook of Organic Photochemistry*; Scianio, J. C., Ed.; CRC Press: Boca Raton, FL, 1989; Vol. 2, pp 3–11.
- Newcomb, M.; Tanaka, N.; Bouvier, A.; Tronche, C.; Horner, J. H.; Musa, O. M.; Martinez, F. N. *J. Am. Chem. Soc.* **1996**, *118*, 8505–8506.
- Hollis, R.; Hughes, L.; Bowry, V. W.; Ingold, K. U. *J. Org. Chem.* **1992**, *57*, 4284–4287.
- Newcomb, M.; Johnson, C. C.; Manek, M. B.; Varick, T. R. *J. Am. Chem. Soc.* **1992**, *114*, 10915–10921.
- Martin-Esker, A. A.; Johnson, C. C.; Horner, J. H.; Newcomb, M. *J. Am. Chem. Soc.* **1994**, *116*, 9174–9181.
- Halgren, T. A.; Roberts, J. D.; Horner, J. H.; Martinez, F. N.; Tronche, C.; Newcomb, M. *J. Am. Chem. Soc.* **2000**, *122*, 2988–2994.
- Alam, M. M.; Watanabe, A.; Ito, O. *J. Org. Chem.* **1995**, *60*, 3440–3444.
- Chatgililoglu, C.; Newcomb, M. *Adv. Organometal. Chem.* **1999**, *44*, 67–112.
- Newcomb, M.; Kaplan, J. *Tetrahedron Lett.* **1987**, *28*, 1615–1618.
- Riddick, J. A.; Bunger, W. B.; Sakano, T. K. *Organic Solvents: Physical Properties and Methods of Purification*, 4th ed.; Techniques of Chemistry, Vol. II; Wiley: New York, 1986.
- Marcus, Y. *Pure Appl. Chem.* **1990**, *62*, 139–147.
- Reichardt, C. *Chem. Rev.* **1994**, *94*, 2319–2358.
- Walbinder, M.; Wu, J. Q.; Fischer, H. *Helv. Chim. Acta* **1995**, *78*, 910–924.
- Zytowski, T.; Fischer, H. *J. Am. Chem. Soc.* **1996**, *118*, 437–439.
- Horner, J. H.; Martinez, F. N.; Musa, O. M.; Newcomb, M.; Shahin, H. E. *J. Am. Chem. Soc.* **1995**, *117*, 11124–11133.
- Chatgililoglu, H.; Crich, D.; Komatsu, M.; Ryu, I. *Chem. Rev.* **1999**, *99*, 1991–2069.
- Tronche, C.; Martinez, F. N.; Horner, J. H.; Newcomb, M.; Senn, M.; Giese, B. *Tetrahedron Lett.* **1996**, *37*, 5845–5848.
- Beckwith, A. L. J.; Bowry, V. W.; Ingold, K. U. *J. Am. Chem. Soc.* **1992**, *114*, 4983–4992.
- Izgorodina, E. I.; Brittain, D. R. B.; Hodgson, J. L.; Krenske, E. H.; Lin, C.-Y.; Namazian, M.; Coote, M. L. *J. Phys. Chem. A* **2007**, *111*, 10754–10768.
- Roschek, B.; Tallman, K. A.; Rector, C. L.; Gillmore, J. G.; Pratt, D. A.; Punta, C.; Porter, N. A. *J. Org. Chem.* **2006**, *71*, 3527–3532.